Exit lane allocation with the lane-based signal optimization method at isolated intersections

Qinrui Tang[1]

Institute of Transportation Systems,

German Aerospace Center (DLR), Berlin, Germany.

Email: qinrui.tang@dlr.de

Alexander Sohr

Institute of Transportation Systems,

German Aerospace Center (DLR), Berlin, Germany.

Email: alexander.sohr@dlr.de

Word count: 5032 Words + 15 Figures/Tables = 8782 Words

[1]Corresponding author.

Abstract

In signal optimization problems, incompatible movements usually are in either of two states: predecessor or successor. However, if the exit lane is well allocated, the incompatible movements merging at the same destination arm can exist in parallel. The corresponding longer green duration is expected to increase the capacity of intersection. This paper aims to solve the exit lane allocation problem with the lane-based method by applying the three states among incompatible movements at conventional signalized intersections. After introducing auxiliary variables, the problem is formulated as a mixed integer programming and can be solved using a standard branch-and-cut algorithm. In addition to the exit lane allocation results, this proposed method can also determine the cycle length, green duration, start of green and signal sequence. The results show that the proposed method can obtain a higher capacity than that without the exit lane allocation. The pavement markings are further suggested for safety.

Key words: signal optimization, exit lane allocation, lane-based method, signal timing plan

1 Introduction

Signal optimization is one of solutions to increase traffic capacities in urban, and the methods of signal optimization thereby attract research interests. The traditional stage-based method, in which a stage is a combination of non-conflict movements having the right of way at the same green time, was developed decades years ago. The widely-used objective of the stage-based method is to minimize the total delay at the intersection (e.g. Webster (1958)), but the multiobjective problem which combines efficiency and safety is also solved in recent years (Li and Sun 2018, 2019). The stage-based method determines the green time (Webster 1958; HBS 2001; Ceylan and Bell 2004), or green split (Al-Khalili 1985), cycle length (Webster 1958; HBS 2001; Ceylan and Bell 2004) or even stage sequence (Memoli et al. 2017; Tang and Friedrich 2018) for given stages in a signal cycle, which means that the stage composition should be done before signal timing optimization. To integrate to stage composition and signal timing optimization, researchers developed the group-based method (Improta and Cantarella 1984; Gallivan and Heydecker 1988; Silcock 1997), in which the given lane markings can be flexiblely "grouped" and their signal timing can be optimized in one mathematical model. However, both the stage-based method and the group-based method require lane markings as exogenous inputs whereas the lane markings could not be always available.

For the purpose of flexibly handling the lane markings, the lane-based method is developed by maximizing the reserved capacity or minimizing the cycle length or the total delay at isolated intersections (Wong and Wong 2003; Wong, Wong and Tong 2006). Wong and Heydecker (2011) then extend the lane-based method via relaxing the numbers of approach lane in traffic arms so that the number of approaching lanes and the exit lanes can be optimized. To better handle the fluctuation of traffic demands, Zhao et al. (2013), Alhajyaseen et al. (2017) and Assi and Ratrout (2018) solved a dynamic lane assignement problem which can automatically determine lane marings based on varied demands, but focus on approaching lanes. To explore the potential application of the lane-based method in the networks, Lee, Wong and Li (2015) and Lee and Wong (2017) estimate the queue length for the intersections with signal control solved by the lane-based method. Meanwhile, the lane-based method is applied for the signal design of unconventional intersections. Signalized roundabouts (Ma et al. 2013), displaced left turn intersections (Zhao et al. 2015), special width approach (Zhao, Liu and Wang 2016) and lane dynamical exclusive bus lane design at intersections (Zhao and Zhou 2018) well adjust the lane-based method into different unconventional intersection designs.

The signal sequence determination in a one-step model is another advantage additional to the lane markings. Signal sequence is affected by the conflict matrix indicating the compatibility between two movements. The compatible movements do not mutually conflict, whereas the incompatible movements do. The incompatibility occurs either at intersections or in the arms where two movements merge at the same destination arms. Thus, for the safety reasons, the incompatible movements must not be in the same green duration to avoid the conflicts. That is, a movement can only be the predecessor or successor of its incompatible movements in a signal cycle, and once it is the predecessor of the incompatible movements, it is not the successor (Wong and Wong 2003). It may result in the possible inefficient utilization of intersection capacities. The conflicts in the destination arms can be eliminated by appropriately allocating exit lanes. In Figure 1, the incompatible movements to the same destination arm can be assigned to different exit lanes so that the conflicts are eliminated. Then the green duration of the related movements could increase so as their capacities. Observing this phenomenon, Xie and Jiang (2016) extend the method of Wong and Heydecker (2011)'s by allocating the exit lanes to turning movements. They group the incompatible movements into strictly incompatible movements referring to the movements going to different destination arms, and potential incompatible movements referring to the movements going to the same destination arm. They draw the conclusion that exit lane allocation can increase the intersection capacity.

[Figure 1 about here.]

When one determines the signal sequence, the incompatible movements can usually be in one of two states: predecessor or successor (e.g. Wong and Wong (2003); Xie and Jiang (2016)). However, the incompatible movements merging at the same destination arm could be in parallel by appropriately allocating the exit lanes. This means, in the previous research, the signal sequence states, predecessor or successor, may not be consistent with the actual situation due to the feasibility of "in parallel". Further, the compatible movements could also be in the one of three states. Thus, the signal sequence variables, which can describe three states referring to predecessor, in parallel or successor rather than the binary states referring to predecessor or successor as Xie and Jiang (2016) did, can more precisely reflect the states of signal sequences, especially for the incompatible movements merging at the same destination.

In this paper, we propose a new method to solve the exit lane allocation problem in the lane-based method to maximize capacities for intersections. The proposed optimization method is developed based on Wong and Wong (2003) which can determine the lane markings of the approaching lanes, the green duration for each lane and for each movement, starts of green for each lane and for each movement, cycle length, signal sequence, assigned flows and reserved capacity. Additional to these decision variables, the exit lane permission indicators are introduced to determine the exit lane allocation. However, the signal sequence variables with three states make the modeling linearization be a challenge. To linearize the model, we introduce two auxiliary binary variables which are explained in the next section in detail. Therefore, the proposed model is formulated as a mixed integer linear programming such that can be efficiently solved with a standard algorithm such as a branch-and-cut algorithm with ILOG CPLEX. Taking maximization of the reserved capacity as the objective function, one can observe the capacity increase by allocating the exit lanes compared with the results of Wong and Wong (2003). Considering the potential conflicts at merging movements, we further suggest the pavement markings to ensure safety.

2 Problem formulation

2.1 Intersection representation

An isolated intersection has N_A arms. In each arm there are L_i approaching lanes and E_i exit lanes, where i is the arm index and $i = 1, ..., N_A$. The turning movements are belong to the direction set M and M contains the elements RT, TH, LT where RT is right turn, TH is through movement, and LT is left turn. In this paper, U-turn is not considered. A movement can be represented as $(i, j), \forall i = 1, ..., N_A, j \in M$ which means a turning direction j in arm i. Meanwhile, a movement can also be represented as a movement from arm $i, i = 1, ..., N_A$ to arm $i', i' = 1, ..., N_A$ and $i \neq i'$. Thus, a relation between the turning direction and the destination arm must hold: $i' = \Gamma(i, j)$. This function means that i' is the destination arm of movement (i, j). The details of the arm index, the approaching lane index and the exit lane index can be found in Figure 2.

[Figure 2 about here.]

2.2 Decision variables

The proposed model can optimize lane markings for approaching lanes, exit lane allocation, signal sequences and signal timing. The decision variables are thereby relevant to these implementation requirements.

Approaching lane permission indicators, $\delta_{i,j,k}$, indicate whether the lane marking of the movement (i, j) is drawn on the approaching lane k. For all $i = 1, ..., N_A, j \in M, k = 1, ..., L_i$, if $\delta_{i,j,k} = 1$, the lane marking of the movement (i, j) is permitted on the approaching lane k; if $\delta_{i,j,k} = 0$, otherwise. Similarly, exit lane permission indicators, $\epsilon_{i,i',k'}$, indicate whether a movement from arm i to arm i' is permitted to exit the intersection via the exit lane k'. For all $i = 1, ..., N_A, i' = 1, ..., N_A, i' \neq i, k' = 1, ..., E_{i'}$, if $\epsilon_{i,i',k'} = 1$, the movement is permitted on the exit lane k'; if $\epsilon_{i,i',k'} = 0$, otherwise. Sequence indicator represents the sequence relationship between different movements. Sequence indicators between movement (i, j) and (l, m) are denoted as $\Omega_{i,j,l,m}$ where $i, l = 1, ..., N_A, j, m \in M$:

$$\Omega_{i,j,l,m} = \begin{cases} 1, & \text{if } (i,j) \text{ is the predecessor of } (l,m) \\ 0, & \text{if } (i,j) \text{ and } (l,m) \text{ are in parallel} \\ -1, & \text{if } (i,j) \text{ is the successor of } (l,m) \end{cases} . \quad (1)$$

To linearize the model, we introduce two auxiliary binary variables $x_{i,j,l,m}, y_{i,j,l,m}, \forall i, l = 1, ..., N_A, j, m \in M$. If $\Omega_{i,j,l,m} \geq 1$, $x_{i,j,l,m} = 0$; $\Omega_{i,j,l,m} < 1$, $x_{i,j,l,m} = 1$. If $\Omega_{i,j,l,m} \geq 0$, $y_{i,j,l,m} = 1$; $\Omega_{i,j,l,m} < 0$, $y_{i,j,l,m} = 0$. Thus, if $x_{i,j,l,m} = 0, y_{i,j,l,m} = 1$, the movement (i, j) is the predecessor of movement (l, m); if $x_{i,j,l,m} = 1, y_{i,j,l,m} = 1$, the movement (i, j) and the movement (l, m) are in parallel; if $x_{i,j,l,m} = 1, y_{i,j,l,m} = 0$, the movement (i, j) is the successor of the movement (l, m). Summarily, $\forall i, l = 1, ..., N_A, j, m \in M$, the following relations hold for the sequence indicators and the auxiliary variables:

$$0 \leq 1 - \Omega_{i,j,l,m} \leq Hx_{i,j,l,m}, \tag{2}$$

$$-1 - H(1 - x_{i,j,l,m}) \leq \Omega_{i,j,l,m} \leq H(1 - x_{i,j,l,m}), \tag{3}$$

$$0 \leq 1 + \Omega_{i,j,l,m} \leq Hy_{i,j,l,m}, \tag{4}$$

$$-H(1 - y_{i,j,l,m}) \leq \Omega_{i,j,l,m} \leq H(1 - y_{i,j,l,m}) + 1, \tag{5}$$

$$x_{i,j,l,m} + y_{i,j,l,m} \geq 1, \tag{6}$$

where H is an arbitrary large positive constant.

Assigned flow $q_{i,j,k}$ is the number of vehicles in the movement (i, j) turning via lane k. The signal timing decision variables include cycle length, green duration and starts of green. The cycle length ξ is formulated as the reciprocal of the actual cycle length for the purpose of linearization. Thus, the actual cycle length is obtained with $1/\xi$. The green duration of a movement $\phi_{i,j}$, the start of green of a movement $\theta_{i,j}$, the green duration of a lane $\Phi_{i,K}$ and the start of green of a lane $\Theta_{i,k}$ are the fraction of the actual cycle length. Hence, the actual green duration of a movement, the actual start of green of a movement, the actual green duration of a lane and the actual start of green of a lane are $\phi_{i,j}/\xi$, $\theta_{i,j}/\xi$, $\Phi_{i,k}/\xi$ and $\Theta_{i,k}/\xi$, respectively.

For simplification, in this paper, the reciprocal of the actual cycle length and the fractions are directly called cycle length, green duration and starts of green. Reserved capacity in this paper is a common flow multiplier which indicates whether the intersection is overloaded or has reserved capacity. The original definition can be found in Allsop (1972).

Decision variables and their domains are summarized in Table 1. In Table 1, c_{min}, c_{max} and g_{min} are the minimum cycle length, maximum cycle length and minimum green duration, respectively.

[Table 1 about here.]

Optionally, if the signal timing of the pedestrian movements needs to be optimized, the relevant decision variables are initialized. They are green duration for pedestrian ($\phi_{i,0}, \forall i = 1, ..., N_A$), start of green for pedestrian ($\theta_{i,0}, \forall i = 1, ..., N_A$), signal sequence for pedestrian ($\Omega_{i,j,i,0}, \Omega_{i,0,i,j}, \Omega_{l,m,i,0}, \Omega_{i,0,l,m}, \forall i, l = 1, ..., N_A, j, m \in M, (i,j) \neq (l,m), i = \Gamma(l,m)$) and the relative auxiliary variables which are similar as the decision variables and the auxiliary variables between movements.

2.3 Objective function

The objective is to maximize the reserved capacity, μ, because the goal of this paper is to gain capacity by allocating the exit lanes. If $\mu > 1$, the intersection has reserved capacity with $100(\mu - 1)$ percent; if $\mu < 1$, the intersection is overloaded with $100(1 - \mu)$ percent. The objective function is

$$\max \mu, \tag{7}$$

subject to the relations (2) - (6) and the constraints (8) - (23). If pedestrian movements are considered, constraints (24) - (31) need to be added as well.

2.4 Constraints

The constraints for the vehicle movements adjusted to our model are explained in detail in constraints (8) - (16) whereas the constraints from the original lane-based method developed by Wong and Wong (2003) are briefly summarized in constraints (17) - (23), followed by the constraints about pedestrian movements.

2.4.1 Minimum and maximum number of permitted lanes

Each movement (i, j) must occupy at least one approaching lane. Meanwhile, the number of permitted lanes for movement (i, j), is less than or equal to the number of exit lanes of the movement; otherwise, vehicles on that movement merging into fewer lanes may cause safety problems (Wong and Wong 2003).

For all $i' = \Gamma(i, j)$, the following constraint holds:

$$1 \leq \sum_{k=1}^{L_i} \delta_{i,j,k} \leq \sum_{k'=1}^{E_{i'}} \epsilon_{i,i',k'}, \forall i, i' = 1, ..., N_A, i' \neq i, j \in M. \tag{8}$$

2.4.2 Conflict elimination on adjacent lanes

The movements on adjacent approaching lanes and exit lanes may conflict with each other. The conflicts must be eliminated for safety reasons (Wong and Wong 2003). Figure 3 is an example of conflicts generated on the adjacent approaching lanes. If a right turn is permitted on lane $k = 2$, the through movement conflict with the left turn on lane $k = 1$ and should not be allowed; if a through movement is permitted on lane $k = 2$, the left turn on the lane $k = 1$ will conflict with the through movement.

[Figure 3 about here.]

To eliminate conflicts in the approaching lanes, the constraint (9) holds. We denote M' as the subset of M. If $j = RT$, $M' = \{TH, LT\}$; if $j = TH$, $M' = \{RT\}$; if $j = LT$, $M' = \emptyset$.

$$\delta_{i,j,k+1} - 1 \leq \delta_{i,m,k} \leq 1 - \delta_{i,j,k+1}, \forall i = 1, ..., N_A, j \in M, k = 1, ..., L_i - 1, m \in M'. \tag{9}$$

The conflicts on the adjacent exit lanes must be also eliminated. The conflicts on the adjacent exit lanes only occur when two conflicted movements have the same destination arm and have the signal sequence in parallel. Figure 4 is an example of the conflicts on adjacent exit lanes. If the exit lane $k' = 2$ is permitted for a through movement, the exit lane $k' = 1$ is not allowed for a right turn; if the exit lane $k' = 2$ is permitted for a left turn, the exit lane $k = 1$ is not allowed for a though movement.

[Figure 4 about here.]

Before handling the exit lanes, we denote the conflict matrix as Ψ. $\psi_{i,j,l,m} \in \Psi, \forall i, l = 1, ..., N_A, j, m \in M$. If $\psi_{i,j,l,m} = 1$, it means a conflict exists between movement (i, j) and movement (l,m); if $\psi_{i,j,l,m} = 0$, otherwise. If $\psi_{i,j,l,m} = 1$, for the movements have the same destination arm which means $i' = \Gamma(i, j) = \Gamma(l, m), \forall i' = 1, ..., N_A$, and have the signal sequence in parallel, the constraint (10) holds. According to the definition of the auxiliary binary variables $x_{i,j,l,m}$ and $y_{i,j,l,m}$, when $x_{i,j,l,m} + y_{i,j,l,m} = 2$, movement (i, j) and (l, m) are in parallel. Hence, if $x_{i,j,l,m} + y_{i,j,l,m} = 2$ and the exit lane k' is allocated for movement (i, j), then the exit lane

k'' cannot be allocated for movement (l, m); if the two movements are not in parallel, the exit lane allocation of lane k' does not influence the exit lane allocation of lane k''.

$$\begin{aligned}&\epsilon_{i,\Gamma(i,j),k'} + x_{i,j,l,m} + y_{i,j,l,m} - 3 \leq \epsilon_{l,\Gamma(l,m),k''} \leq 3 - (\epsilon_{i,\Gamma(i,j),k'} + x_{i,j,l,m} + y_{i,j,l,m}),\\ &\forall i, l = 1, ..., N_A, i \neq l, j \in M, m \in M', \Gamma_{i,j} = \Gamma_{l,m},\ k' \text{ and } k'' = 1, ..., E_i, k'' > k'.\end{aligned} \tag{10}$$

2.4.3 Order of signal displays

The conflicts among movements mainly influence the order of signal displays. If two conflict movements have different destination arms, they can be either predecessor or successor of each other. If two conflict movements have the same destination arm, they could be either in parallel or not. If two movements do not conflict with each other, they could be the predecessor or successor or in parallel. Conflict matrix records the conflicts among movements and contributes to the constraint construction.

Althoug in a cycle a signal could appear multiple times so that the signal is both the predecessor and successor of another, this paper limits this case for simplification as this is not that commom in signal planning. Therefore, no matter whether the movements conflict with each other, constraint(11) holds, saying that if one movement is the predecessor of another, another movement can only be the successor of the one; or if one movement is in parallel with another, another movement is also in parallel with the one. Similar constraint can also be found in Wong and Wong (2003).

$$\Omega_{i,j,l,m} + \Omega_{l,m,i,j} = 0, \forall i, l = 1, ..., N_A, i \neq l,\ j \text{ and } m \in M. \tag{11}$$

If $\psi_{i,j,l,m} = 1$, for the movements have different destination arms, i.e. $\Gamma(i,j) \neq \Gamma(l,m)$, they cannot be in parallel. Hence,

$$x_{i,j,l,m} + y_{i,j,l,m} = 1; \forall i, l = 1, ..., N_A, i \neq l,\ j \text{ and } m \in M. \tag{12}$$

If $\psi_{i,j,l,m} = 1$ and the movement (i, j) and the movement (l, m), which have the same destination arm, are in parallel (i.e. $x_{i,j,l,m} = 1, y_{i,j,l,m} = 1$), the exit lane k' can only be assigned for either the movement (i, j) or the movement (l, m) to avoid conflicts; if the movement (i, j) and the movement (l, m) are not in parallel (i.e. $x_{i,j,l,m} + y_{i,j,l,m} = 1$), they cannot conflict with each other, so it does not matter that the exit lane k' is assigned for which movements.

$$\begin{gathered}\epsilon_{i,i',k'} + \epsilon_{l,i',k'} \leq 3 - (x_{i,j,l,m} + y_{i,j,l,m}),\\ \forall i, l = 1, ..., N_A, i \neq l, i' = \Gamma(i, j) = \Gamma(l, m),\ j, m \in M, k' = 1, ..., E_{i'}.\end{gathered} \tag{13}$$

2.4.4 Identical signal sequence on shared approaching lanes

When two movements share the same lane, the signal sequence between the two movements and the other movements must be the same to avoid internal conflicts on the lanes. Thus, if movement (i, j) and (i, j') are permitted on the approaching lane k, the values of their signal sequence indicator must be the same.

$$\begin{gathered}\delta_{i,j,k} + \delta_{i,j',k} - 2 \leq \Omega_{i,j,l,m} - \Omega_{i,j',l,m} \leq 2 - (\delta_{i,j,k} + \delta_{i,j',k}),\\ \forall i, l = 1, ..., N_A, i \neq l,\ j, j', m \in M, j' > j, k = 1, ..., L_i.\end{gathered} \tag{14}$$

2.4.5 Clearance time

If two movements are predecessor/successor of each other, there is at least a clearance time in-between the green duration of the movements due to potential safety problems. Thus, if the movement (i, j) is the predecessor of the movement (l, m), then $x_{i,j,l,m} = 0, y_{i,j,l,m} = 1$, and the start of green of the movement (l, m) must be later than the sum of the start of green and the green duration of the movement (i, j) and the clearance time (See constraint(15)); if the movement (i, j) is the successor of the movement (l, m), then $x_{i,j,l,m} = 1, y_{i,j,l,m} = 0$, and the constraint(16) holds.

$$\theta_{i,j} + \phi_{i,j} + \omega_{i,j,l,m}\xi \le \theta_{l,m} + x_{i,j,l,m}, \forall i, l = 1, ..., N_A, i \ne l,\ j, m \in M. \tag{15}$$

$$\theta_{l,m} + \phi_{l,m} + \omega_{l,m,i,j}\xi \le \theta_{i,j} + y_{i,j,l,m}, \forall i, l = 1, ..., N_A, i \ne l,\ j, m \in M. \tag{16}$$

2.4.6 Constraints from the original lane-based method

This section includes the constraints from Wong and Wong (2003)' model. Considering better readability of this paper, we summarize the constraints below and apply a brief explanation. More details can be found in Wong and Wong (2003).

$$\sum_{j \in M} \delta_{i,j,k} \ge 1, \forall i = 1, ..., N_A; k = 1, ..., L_i, \tag{17}$$

$$-H(1 - \delta_{i,j,k}) \le \Phi_{i,k} - \phi_{i,j} \le H(1 - \delta_{i,j,k}), \forall i = 1, ..., N_A, j \in M, k = 1, ..., L_i, \tag{18}$$

$$-H(1 - \delta_{i,j,k}) \le \Theta_{i,k} - \theta_{i,j} \le H(1 - \delta_{i,j,k}), \forall i = 1, ..., N_A, j \in M, k = 1, ..., L_i, \tag{19}$$

$$\mu Q_{i,j} = \sum_{k=1}^{L_i} q_{i,j,k}, \forall i = 1, ..., N_A, j \in M, \tag{20}$$

$$q_{i,j,k} \le H\delta_{i,j,k}, \forall i = 1, ..., N_A, j \in M, k = 1, ..., L_i, \tag{21}$$

$$\begin{gathered} -H(2 - \delta_{i,j,k} - \delta_{i,j,k+1}) \le \upsilon_{i,k} - \upsilon_{i,k+1} \le H(2 - \delta_{i,j,k} - \delta_{i,j,k+1}), \\ \forall i = 1, ..., N_A, j \in M, k = 1, ..., L_i - 1, \end{gathered} \tag{22}$$

$$u_{i,k} = \frac{\upsilon_{i,k}}{\Phi_{i,k} + e\xi} \le u_{max,i,k}, \forall i = 1, ..., N_A, k = 1, ..., L_i, \tag{23}$$

where H is an arbitrary large positive constant, $\upsilon_{i,k} = \sum_{j\in M} \frac{q_{i,j,k}}{s_j}$ is flow factor of lane k in arm i, s_j is the saturation flow of movements on exclusive lanes, e is the difference between actual green time and effective green time and predefined as 1 s, and $u_{max,i,k}$ is the maximum acceptable degree of saturation.

Due to the completeness principle of signal timing plan design, all movements should be included in the signal cycle, so constraint (17) holds. Signal timing is the most important issue to be solved. When more than one movements share one lane, the signal settings of these movements are identical to avoid internal conflict on the lane (constraint (18) and (19)). Traffic flows must be treated as well which refers to constraint (20) - (23). The maximum amount of traffic increase, which confirms the reasonable performance of the intersection, is the product of reserved capacity μ and demands $Q_{i,j}$. The maximum amount is equal to the sum of traffic flows of movement (i, j) being assigned to all lanes on arm i (constraint (20)). The assigned flow $q_{i,j,k}$ must be 0 if movement (i, j) is not permitted on lane k (constraint (21)). If two movements share the same lane and two adjacent lanes are permitted, the degree of saturation on both lanes is identical, resulting in equal flow factors, for signal settings of these adjacent lanes are the same (constraint (22)). The degree of saturation should be no more than the maximum acceptable degree of saturation (constraint (23)).

2.4.7 Pedestrian movement

If the decision variables of pedestrian movements need to be determined, the constraints for the signal sequence and the clearance time will be handled. However, firstly all relevant decision variables must be in their domain.

$$0 \leq \theta_{i,0} \leq 1, \forall i = 1, ..., N_A, \tag{24}$$

$$g_{min,0}\xi \le \phi_{i,0} \le 1, \forall i = 1, ..., N_A, \tag{25}$$

where $g_{min,0}$ is the minimum green duration for the pedestrian movement.

For each pedestrian movement, it can conflict with both the movements starting from an arm and the movements ending at the same arm. To distinguish the two cases, we use movement (i, j) as the movement starting at arm i and movement (l, m) as the movement ending at arm i. Similar as the vehicle movements, the auxiliary binary variables, $x_{i,j,i,0}, y_{i,j,i,0}, x_{l,m,i,0}$ and $y_{l,m,i,0}$ are introduced. $\forall i = 1, ..., N_A, j \in M$, if $\Omega_{i,j,i,0} \ge 1$, $x_{i,j,i,0} = 0$; $\Omega_{i,j,i,0} < 1$, $x_{i,j,i,0} = 1$; if $\Omega_{i,j,i,0} \ge 0$, $y_{i,j,i,0} = 1$; $\Omega_{i,j,i,0} < 0$, $y_{i,j,i,0} = 0$. $\forall l = 1, ..., N_A, m \in M, \Gamma(l, m) = i$, if $\Omega_{l,m,i,0} \ge 1$, $x_{l,m,i,0} = 0$; $\Omega_{l,m,i,0} < 1$, $x_{l,m,i,0} = 1$; if $\Omega_{l,m,i,0} \ge 0$, $y_{l,m,i,0} = 1$; $\Omega_{l,m,i,0} < 0$, $y_{l,m,i,0} = 0$. Then $x_{i,j,i,0}, y_{i,j,i,0}, x_{l,m,i,0}$ and $y_{l,m,i,0}$ follow the relations similar as the relations (2) - (6).

For the movement (i, j) starting from arm i,

$$\Omega_{i,j,i,0} + \Omega_{i,0,i,j} = 0, \forall i = 1, ..., N_A, j \in M, \tag{26}$$

$$\theta_{i,j} + \phi_{i,j} + \omega_{i,j,i,0}\xi \le \theta_{i,0} + x_{i,j,i,0}, \forall i = 1, ..., N_A, j \in M, \tag{27}$$

$$\theta_{i,0} + \phi_{i,0} + \omega_{i,0,i,j}\xi \le \theta_{i,j} + y_{i,j,i,0}, \forall i = 1, ..., N_A, j \in M. \tag{28}$$

For the movement (l, m) merging at arm i,

$$\Omega_{l,m,i,0} + \Omega_{i,0,l,m} = 0, \forall i, l = 1, ..., N_A, m \in M, i = \Gamma(l, m), \tag{29}$$

$$\theta_{l,m} + \phi_{l,m} + \omega_{l,m,i,0}\xi \le \theta_{i,0} + x_{l,m,i,0}, \forall i, l = 1, ..., N_A, m \in M, i = \Gamma(l, m), \tag{30}$$

$$\theta_{i,0} + \phi_{i,0} + \omega_{i,0,l,m}\xi \le \theta_{l,m} + y_{l,m,i,0}, \forall i, l = 1, ..., N_A, m \in M, i = \Gamma(l, m), \tag{31}$$

where $\omega_{i,j,i,0}, \omega_{i,0,i,j}, \omega_{l,m,i,0}$ and $\omega_{i,0,l,m}$ are the clearance time.

3 Numerical examples

3.1 Numerical configurations

The layout of the studied intersection can be found in Figure 2 whereas the number of approaching lanes and exit lanes vary according to Table 2, which summarizes the details of the number of approaching lanes and exit lanes for each intersection.

[Table 2 about here.]

Additional to the configurations of studied intersections, traffic demand, conflict matrix, saturation flows for each movement and the values of bounds for signal timing have to be given. The traffic demand and the conflict matrix can be seen in Table 3 and Table 4, respectively. In this section, only protected left turns are used. If permitted left turns could be present, the conflicts between left turns and the opposing through movements and the conflicts between left turns and the opposing right turns should be marked as 0 in Table 4. However, the optimal result could show that the "permitted left turns" are not in the same green duration as their opposing through movement because compatible movements could be in different green duration, and then the left turns are actually protected. According to HCM (2000), the saturation flow of through movement is assigned as 1900 veh/h; the saturation flow of right turn is 1615 veh/h; the saturation flow of left turn is 1805 veh/h. The cycle length is within the range of 60 s and 90 s. The green duration for all movements must be no less than 5 s. The clearance time between conflicted movements is 5 s. The maximum acceptable degrees of saturation, $u_{max,i,k}, \forall i = 1, ..., N_A, k = 1, .., L_i$, are assigned as 90%.

For the purpose of observation of the capacity increase, we compare our proposed model with a reference model which is developed by Wong and Wong (2003) whereas the signal timing for pedestrian movements is excluded as the focus of this paper is the exit lane allocation for vehicles. The reference model and the proposed model are implemented in Java integrated with ILOG CPLEX 12.8 which is a professional solver for the linear programming. The PC, whose CPU is Intel Core i7 with 2.7GHz and memory is 16.0GB, performs the numerical example.

[Table 3 about here.]

[Table 4 about here.]

3.2 Overall optimization results

Table 5 summarizes the overall optimization results for both the reference model and the proposed model so that their optimization results can be better compared. The number of variables and the number of constraints represent the problem sizes of the models. The problem size of the proposed model is larger than the problem size in the reference model, but the proposed model can still be efficiently solved. The optimal reserved capacities increase as the number of approaching lanes and the number of exit lanes increase. With the positive values of μ (see Column 8), all intersection have reserved capacity which can be found in Column 9. The capacity increase due to the exit lane allocation is in the final column of Table 5. Compared to the reference model, the capacity increase for intersection 1, 2, 3 and 4 is 1.14%, 9.23%, 9.23% and 13.23%, respectively. This means that appropriately allocating the exit lanes can increase the capacity, and as the number of approaching lanes and the number of exit lanes increase, the capacity increase goes larger.

[Table 5 about here.]

3.3 Signal timing plan and lane allocation

Signal timing plan reflects the results of cycle length, green duration, and starts of green and signal sequences. Lane allocation reflects the results of approaching lane permission and exit lane allocation. Signal timing plan and lane allocation are demonstrated in this section together because the link between the signal timing and lane allocation can be clearly built. By maximizing the reserved capacity, the cycle length for all intersections is 90 s. The signal timing plan for each intersection is shown in Figure 5(a), Figure 6(a), Figure 7(a) and Figure 8(a), respectively. In each signal timing plan, there are green duration which incompatible movements have the right-of-way at the same time. The green duration is numbered at the bottom of the signal timing plans. Therefore, Figure 5(b), Figure 6(b), Figure 7(b) and Figure 8(b) display how the incompatibility is eliminated for each intersections, respectively. The lane markings, i.e. the approaching lane allocation, can also be found in these figures.

At intersection 1, the conflicts of incompatible movements in four intervals of green duration are eliminated (see Figure 5(b)). In the first green duration, the though movement from arm 2 goes to the exit lane 2 and 3 in arm 4, and the left turn from arm 3 goes to the exit lane 1, so they do not conflict. The clearance time between these two movements is then not necessary, which means longer green duration for the relevant movements. Similarly, the elimination of conflicts can be found in the second, the third and the fourth interval of green duration. At intersection 2, there three intervals of green duration for the incompatible movements (see Figure 6(b)). As the exit lane of the right turn from arm 4 can be well allocated, this movement has a full-green duration. Four intervals of green duration for the incompatible movements at intersection 3 can be seen in Figure 7(b). Due to the appropriate exit lane allocation, at this intersection, the right turns from arm 2, arm 3 and arm 4 have a full-green duration as well, and their clearance time is not necessary. Intersection 4 also has four green duration for incompatible movements (see Figure 7(b)). The movements from three arms could be in the green duration at the same time at both intersection 3 and 4 as their number of exit lanes increases.

[Figure 5 about here.]

[Figure 6 about here.]

[Figure 7 about here.]

[Figure 8 about here.]

3.4 Traffic performance measurement

In this section, the assigned flows for each lane are recorded and then lane flows, lane saturation flow, lane capacities and degree of saturation are calculated and shown in Table 6. With these traffic performance measures, we can better evaluate the results. Column 3-6 display the results of assigned flows. Then for each lane, the lane flows can be obtained by summing up the assigned flow by lane (see Column 7). Meanwhile, the lane saturation flow can be calculated according to the assigned flow and the lane flow. The value of lane saturation flow is shown in Column 8. The capacity of the lane in Column 9 is the product of saturation flow and lane green split. Degree of saturation for each lane in Column 10 is then the lane flow divided the capacity. When movements share the same lane, their degrees of saturation are the same and it can be found from the values of the degrees of saturation. As the number of approaching lane increases from intersection 1 to intersection 4, the degree of saturation obviously decreases. However, as intersection 2 and 3 has the same optimal reserved capacity, they have the same value of the performance measures. Right turns benefit from the exit lane allocation, and their degrees of saturation are relatively small. For example, at intersection 2 & 3, the degree of saturation of the right turn in arm 2 (from arm 2 to arm 1) is 0.2594, and the degree of saturation of the right turn in arm 4 (from arm 4 to arm 3) is 0.1238. They are much fewer than the degrees of saturation for the rest movements. That means, they gain capacities due to the exit lane allocation.

[Table 6 about here.]

4 Discussion

We propose a method to solve the exit lane allocation problem as a mixed integer linear programming in the lane-based method. Capacity increases after the exit lanes are suitably allocated for incompatible movements ending at the same destination arm. We apply exit lane indicators and precise sequence states among incompatible movements: predecessor, in parallel and successor, so that extend the lane-based signal optimization method. We would like to discuss the reasons why exit lane allocation can increase capacities and the safety aspect of exit lane allocation.

The incompatible movements require clearance time in-between for safety reasons, but the well allocated exit lanes avoid the conflicts and so as the clearance time. The green duration for related incompatible movements thereby becomes longer, resulting in larger capacities for these movements. It is interesting to notice that the number of exit lanes influence the capacity increase. As the number of exit lanes increases, the capacity increases. Large number of exit lanes allows more approaching lanes for a movement, including the incompatible movements ending at the same destination arm. A large number of approaching lanes for a movement obviously increases the capacity. On another hand, the total green duration of incompatible movements increases from intersection 1 to 4. Longer green duration is another factor to increase the capacity.

To ensure the safety of the exit lanes of incompatible movements ending at the same destination, the design of pavement markings at intersections needs to be considered. The pavement markings can guide drivers to correctly follow a lane to avoid conflicts from the vehicles of their incompatible movements, when they have the right-of-way in the overlapping green duration. Figure 9 shows the pavement markings of all exit lanes of incompatible movements being correctly guided. The standard of pavement marking design in Germany can be found in FGSV (1993). Although our model can get the exit lane allocation for all movements, the exit lane allocation for compatible movements and the incompatible movements in different green duration is less important because they do not mutually conflict. Thus, only the pavement markings of the incompatible movements having overlapping green duration are kept in Figure 9 to reduce the complexity of pavement markings at intersections. However, as the number of lanes increases, the pavement markings still become complicated. We should pay attention on the potential accidents caused by overloaded information of pavement markings.

[Figure 9 about here.]

5 Conclusions

A lane-based signal optimization method integrating the exit lane allocation at isolated intersections is proposed. The proposed method can determine lane markings, exit lane allocation, signal sequences, green duration, starts of green, cycle length, assigned flows and reserved capacity. The precise sequence states referring to predecessor, successor and in parallel are applied. With the linear objective of maximizing the reserved capacity and constraints, this problem is formulated as a mixed integer linear programming, which can be efficiently solved with standard branch-and-cut algorithm. By applying this method, the exit lane allocation for incompatible movements ending at the same destination arm becomes feasible, which is a significant extension on the original lane-based method. Numerical example shows that the appropriate exit lane allocation can gain capacity at intersections. Pavement marking design suggestions also contribute to avoiding accidents in the practical application.

Acknowledgements

This work was supported by the Joint Center of Research for Mobility, Traffic-safety and Environment, by German Aerospace Center (DLR) and Tongji University, which is financially supported by the Germany Ministry of Education and Research (BMBF). The support is gratefully acknowledged.

References

Al-Khalili, Asim J. 1985. "The optimum green split of a cycle time." IEEE Transactions on Systems, Man, and Cybernetics (5):675–681.

Alhajyaseen, Wael KM, Nedal T Ratrout, Khaled J Assi and Amjad Abu Hassan. 2017. "The Integration of Dynamic Lane Grouping Technique and Signal Timing Optimization for Improving the Mobility of Isolated Intersections." Arabian Journal for Science and Engineering 42(3):1013–1024.

Allsop, R. 1972. "Estimating the traffic capacity of a signalized road junction." Transportation Research 6:245–255.

Assi, Khaled J and Nedal T Ratrout. 2018. "Proposed quick method for applying dynamic lane assignment at signalized intersections." IATSS research 42(1):1–7.

Ceylan, Halim and Michael GH Bell. 2004. "Traffic signal timing optimisation based on genetic algorithm approach, including drivers' routing." Transportation Research Part B: Methodological 38(4):329–342.

FGSV. 1993. "Richtlinien für die Markierung von Straßen (RMS, Guidelines for Marking Roads), Teil 1: Abmessung und geometrische Anordnung von Markierungszeichen (RMS-1, Part 1 Dimensions and geometric arrangement of markers).".

Gallivan, Stephen and Benjamin Heydecker. 1988. "Optimising the control performance of traffic signals at a single junction." Transportation Research Part B: Methodological 22(5):357–370.

HBS. 2001. Handbuch für die Bemessung von Straßenverkehrsanlagen (HBS, German Highway Capacity Manual). Cologne, Germany: Road and Transport Association.

HCM. 2000. Highway Capacity Manual. Chapter 16: Signalized Intersections. Washington, DC, the USA: Transportation Research Board (TRB).

Improta, G. and G. E. Cantarella. 1984. "Control system design for an individual signalized junction." Transportation Research Part B 18(2):147–167.

Lee, Seunghyeon and SC Wong. 2017. "Group-based approach to predictive delay model based on incremental queue accumulations for adaptive traffic control systems." Transportation Research Part B: Methodological 98:1–20.

Lee, Seunghyeon, SC Wong and YC Li. 2015. "Real-time estimation of lane-based queue lengths at isolated signalized junctions." Transportation Research Part C: Emerging Technologies 56:1–17.

Li, Xiang and Jian-Qiao Sun. 2018. "Signal Multiobjective Optimization for Urban Traffic Network." IEEE Transactions on Intelligent Transportation Systems (99):1–9.

Li, Xiang and Jian-Qiao Sun. 2019. "Intersection multi-objective optimization on signal setting and lane assignment." Physica A: Statistical Mechanics and its Applications 525:1233–1246.

Ma, Wanjing, Yue Liu, Larry Head and Xiaoguang Yang. 2013. "Integrated optimization of lane markings and timings for signalized roundabouts." Transportation research part C: emerging technologies 36:307–323.

Memoli, Silvio, Giulio E Cantarella, Stefano de Luca and Roberta Di Pace. 2017. "Network signal setting design with stage sequence optimisation." Transportation Research Part B: Methodological 100:20–42.

Silcock, JP. 1997. "Designing signal-controlled junctions for group-based operation." Transportation Research Part A: Policy and Practice 31(2):157–173.

Tang, Qinrui and Bernhard Friedrich. 2018. "Design of Signal Timing Plan for Urban Signalized Networks including Left Turn Prohibition." Journal of Advanced Transportation 2018.

Webster, F. V. 1958. Traffic signal settings. Technical Report Road Research Technical Paper, No.39 Road Research Laboratory, London.

Wong, C. K. and B. G. Heydecker. 2011. "Optimal allocation of turns to lanes at an isolated signal-controlled junction." Transportation Research Part B: Methodological 45(4):667–681.

Wong, C. K. and S. C. Wong. 2003. "Lane-based optimization of signal timings for isolated junctions." Transportation Research Part B: Methodological 37(1):63–84.

Wong, C. K., S. C. Wong and C. O. Tong. 2006. "A Lane-Based Optimization Method for the Multi-Period Analysis of Isolated Signal-Controlled Junctions." Transportmetrica 2(1):53–85.

Xie, Siyang and Hai Jiang. 2016. "Increasing the capacity of signalized intersections by allocating exit lanes to turning movements." Journal of Advanced Transportation 50(8):2239–2265.

Zhao, Jing, Wanjing Ma, H Michael Zhang and Xiaoguang Yang. 2013. "Two-step optimization model for dynamic lane assignment at isolated signalized intersections." Transportation Research Record 2355(1):39–48.

Zhao, Jing, Wanjing Ma, K Larry Head and Xiaoguang Yang. 2015. "Optimal operation of displaced left-turn intersections: A lane-based approach." Transportation Research Part C: Emerging Technologies 61:29–48.

Zhao, Jing and Xizhao Zhou. 2018. "Improving the Operational Efficiency of Buses With Dynamic Use of Exclusive Bus Lane at Isolated Intersections." IEEE Transactions on Intelligent Transportation Systems .

Zhao, Jing, Yue Liu and Tao Wang. 2016. "Increasing signalized intersection capacity with unconventional use of special width approach lanes." Computer-Aided Civil and Infrastructure Engineering 31(10):794–810.

Figures

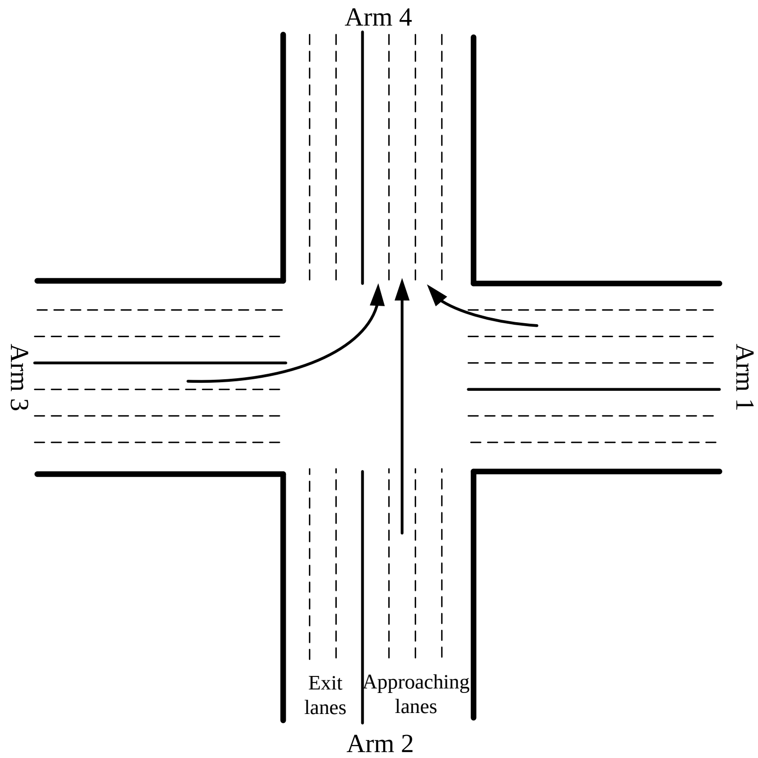

Figure 1: Appropriate exit lane allocation can eliminate the conflicts in destination arms

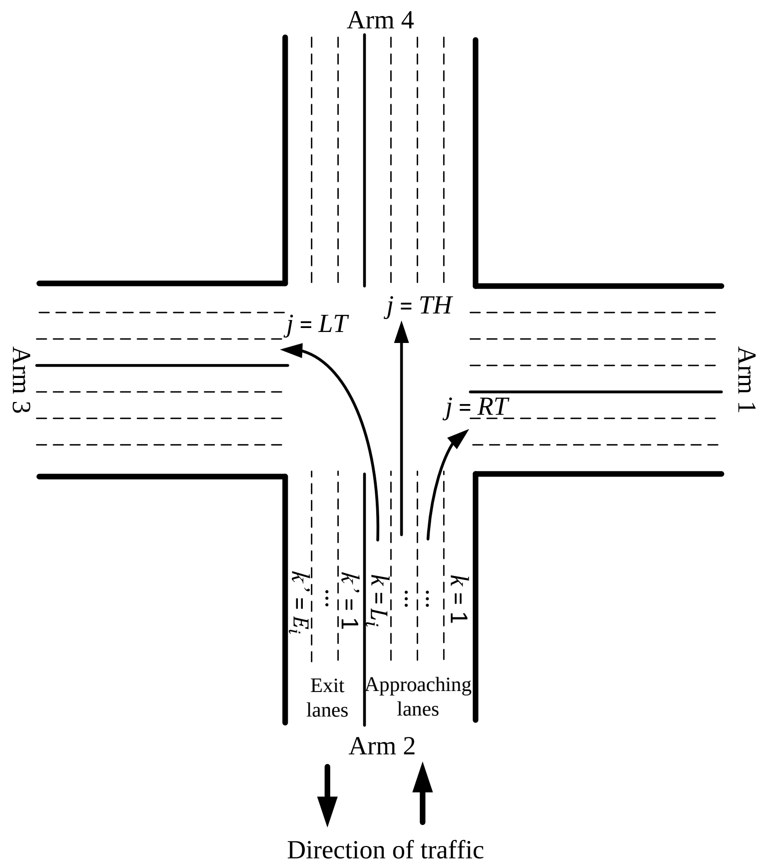

Figure 2: Intersection representation

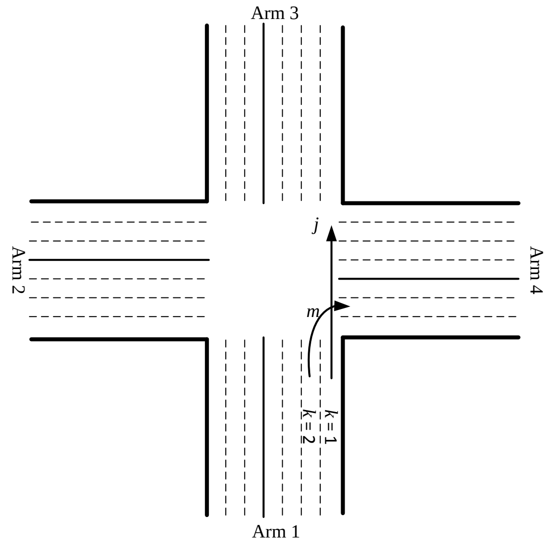

Figure 3: Examples of conflict on adjacent approaching lanes

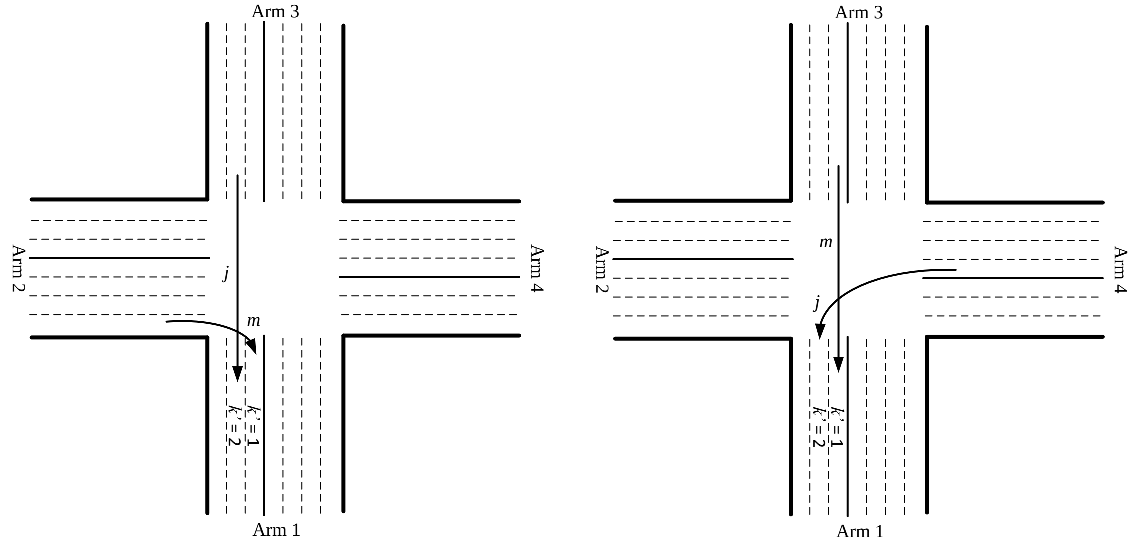

Figure 4: Examples of conflict on adjacent exit lanes

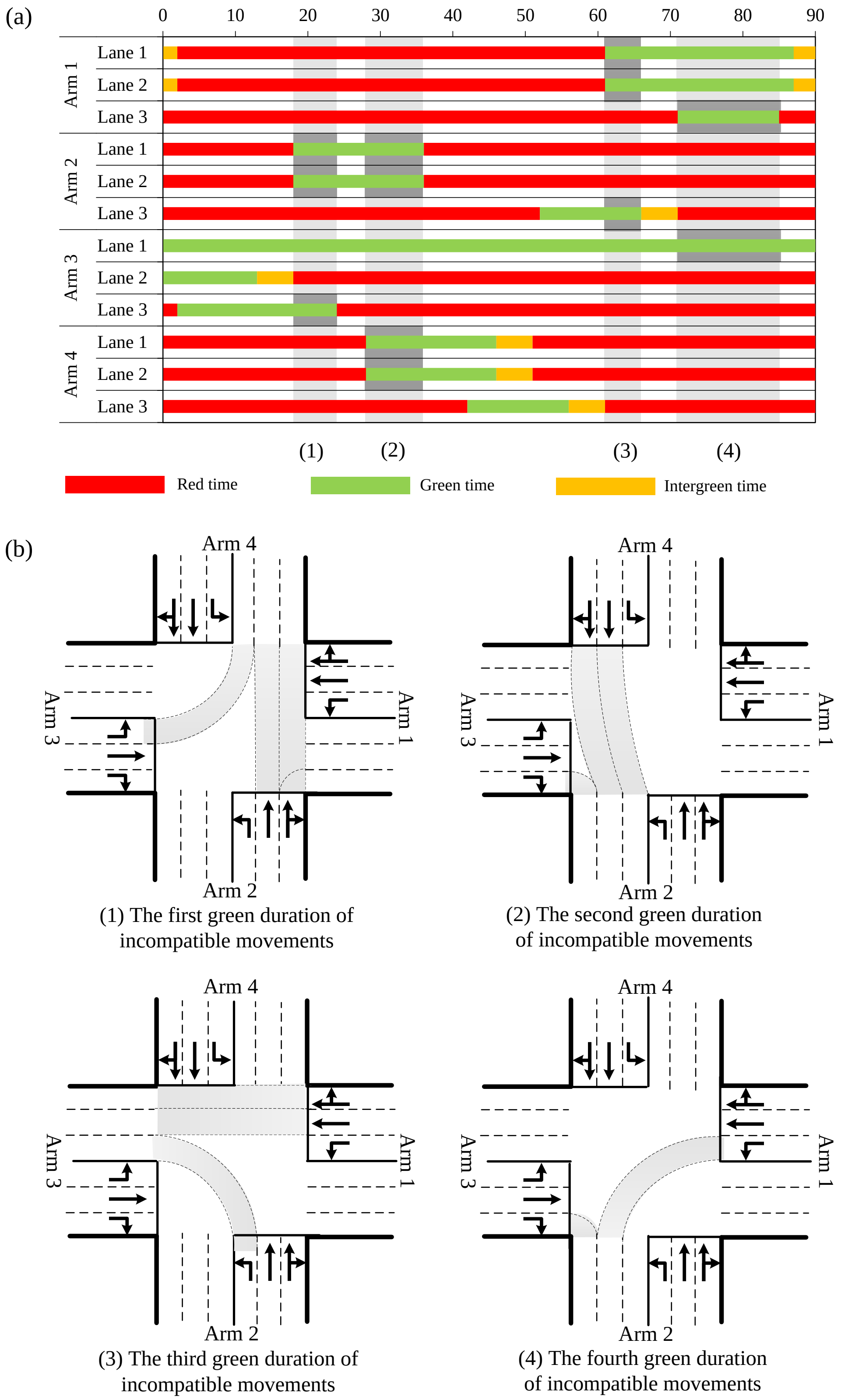

Figure 5: (a) Signal timing plan of intersection 1; (b) Exit lane allocation to eliminate conflicts at intersection 1

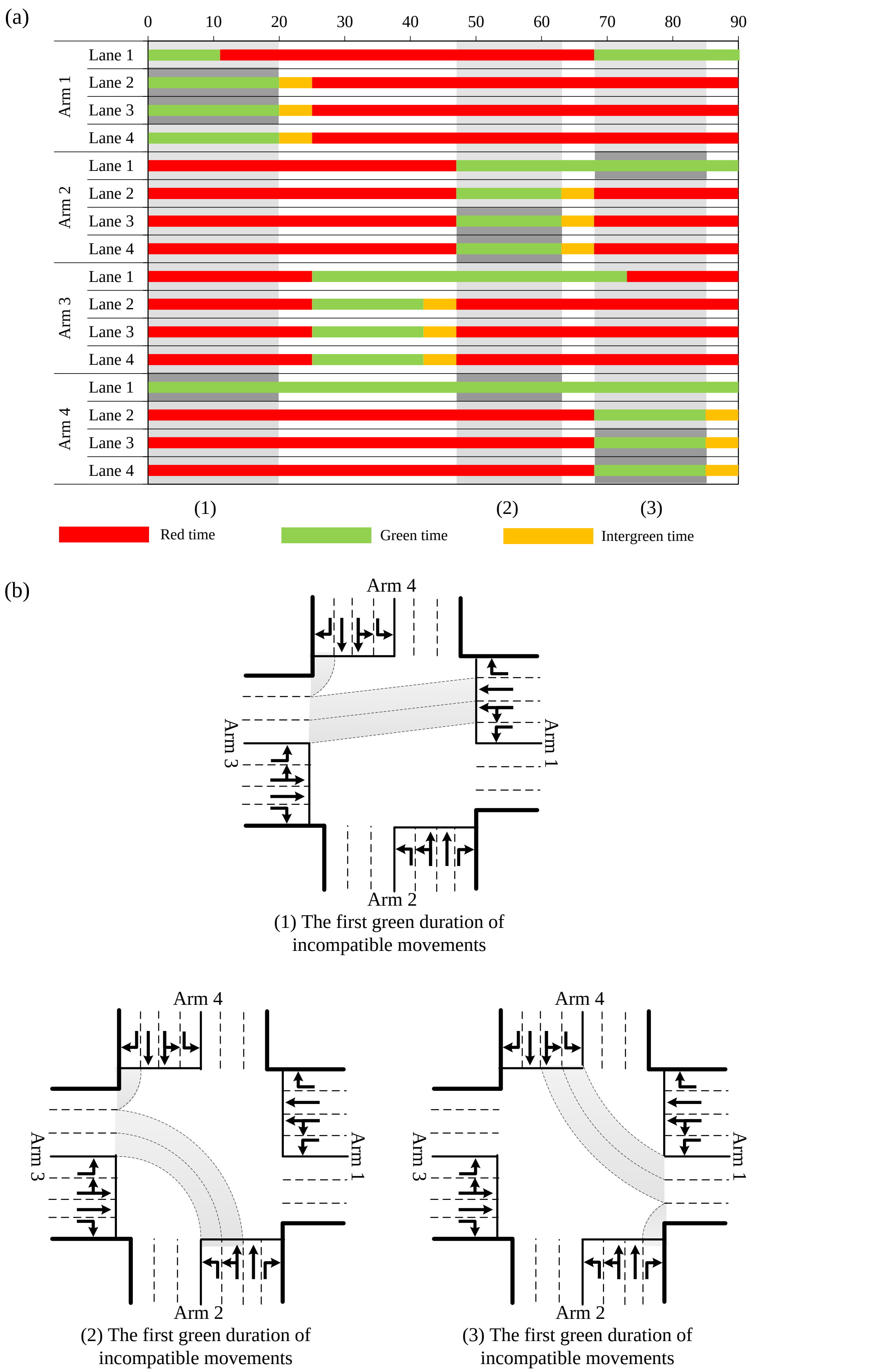

Figure 6: (a) Signal timing plan of intersection 2; (b) Exit lane allocation to eliminate conflicts at intersection 2

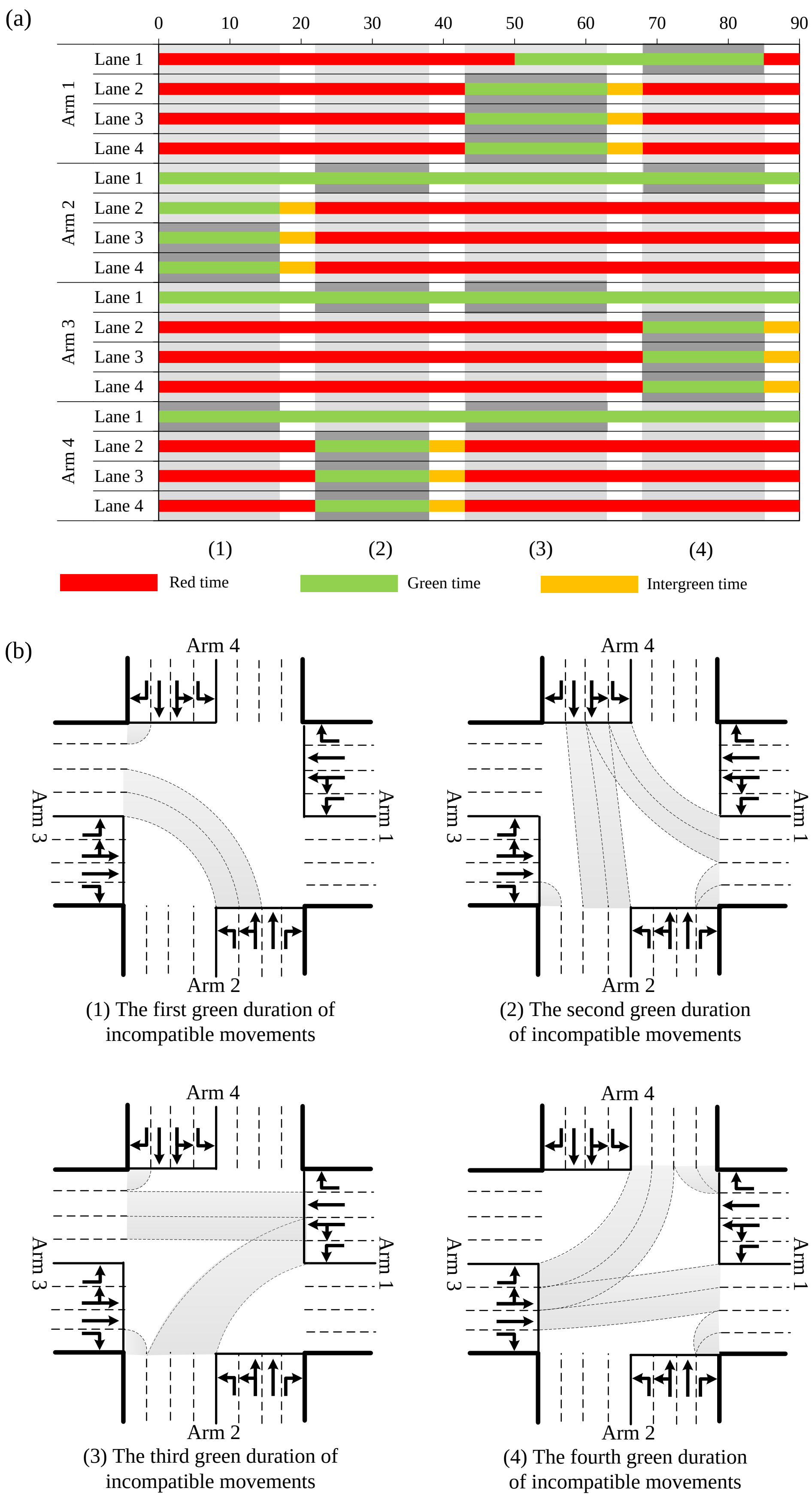

Figure 7: (a) Signal timing plan of intersection 3; (b) Exit lane allocation to eliminate conflicts at intersection 3

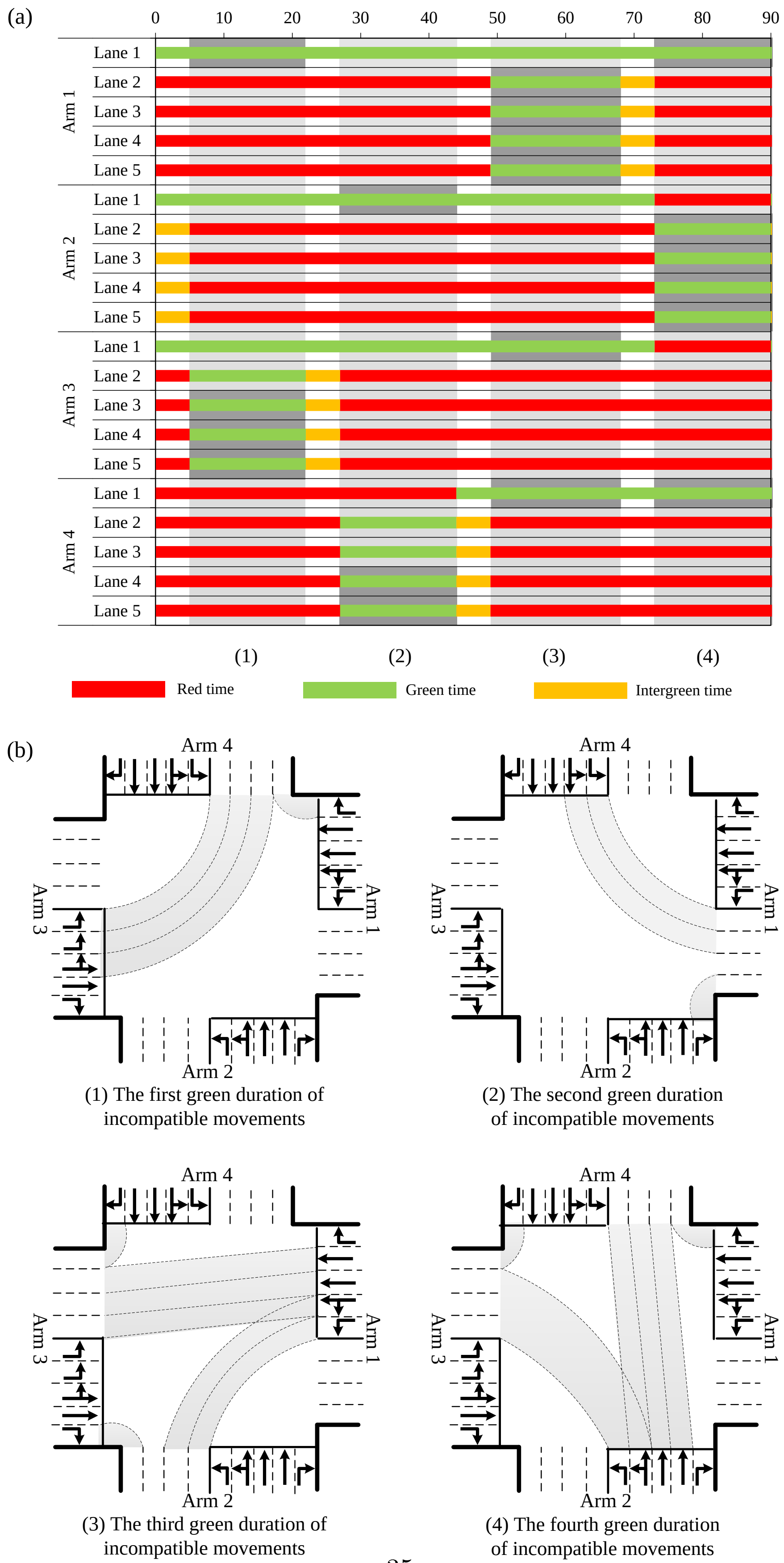

Figure 8: (a) Signal timing plan of intersection 4; (b) Exit lane allocation to eliminate conflicts at intersection 4

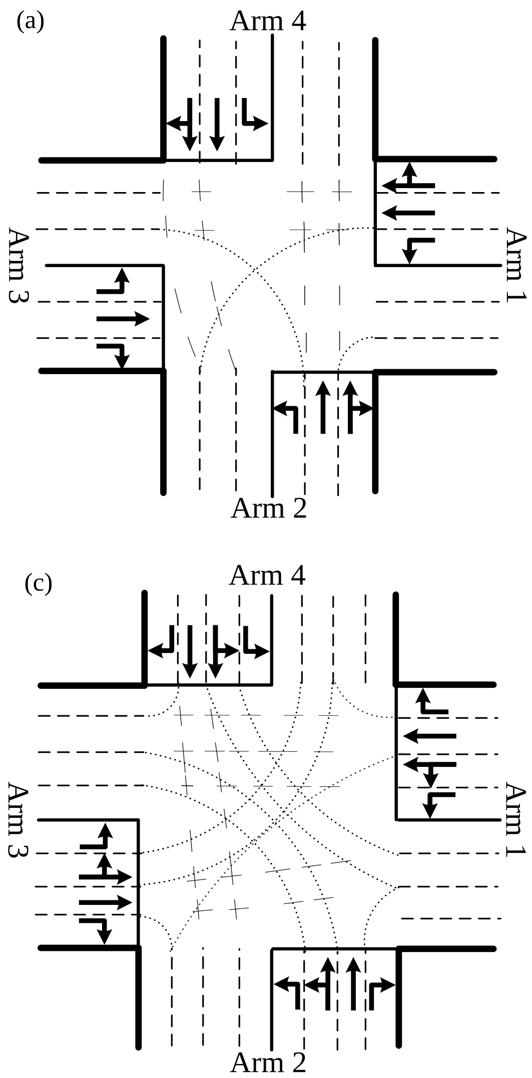

Figure 9: Pavement markings of exit lanes of incompatible movements: (a) Pavement markings of intersection 1; (b) Pavement markings of intersection 2; (c) Pavement markings of intersection 3; (d) Pavement markings of intersection 4

Tables

Table 1: List of decision variables

Decision variables	Notation	Domain
Approaching lane permission indicator	$\delta_{i,j,k}$	$\delta_{i,j,k} \in \{0,1\}$
Exit lane permission indicator	$\epsilon_{i,i',k}$	$\epsilon_{i,j,k} \in \{0,1\}$
Sequence indicator	$\Omega_{i,j,l,m}$	$\Omega_{i,j,l,m} \in \{-1,0,1\}$
Assigned flow of a movement on a lane (veh/h)	$q_{i,j,k}$	$q_{i,j,k} \in [0,\infty)$
Reciprocal of cycle length	ξ	$\xi \in [1/c_{max}, 1/c_{min}]$
Green duration for lane	$\Phi_{i,k}$.	$\Phi_{i,K} \in [g_{min}\xi, 1]$
Start of green for lane	$\Theta_{i,k}$	$\Theta_{i,k} \in [0,1]$
Green duration for movement	$\phi_{i,j}$.	$\phi_{i,j} \in [g_{min}\xi, 1]$
Start of green for movement	$\theta_{i,j}$	$\theta_{i,j} \in [0,1]$
Reserved capacity	μ	$\mu \in [0,\infty)$

Table 2: Studied intersection configuration

Intersection	Number of approaching lanes	Number of exit lanes
1	3	3
2	4	3
3	4	4
4	5	4

Table 3: Traffic demand for studied intersections (veh/h)

	To arm			
From arm	1	2	3	4
1	-	300	400	200
2	200	-	300	200
3	400	200	-	300
4	200	300	200	-

Table 4: Conflict matrix for studied intersections

Arm, i		1			2			3			4		
	Direction, j	RT	TH	LT	RT	TH	LT	RT	TH	LT	RT	TH	LT
	RT	0	0	0	0	1	0	0	0	1	0	0	0
1	TH	0	0	0	0	1	1	0	0	1	1	1	1
	LT	0	0	0	0	1	1	1	1	0	0	1	1
	RT	0	0	0	0	0	0	0	1	0	0	0	1
2	TH	1	1	1	0	0	0	0	1	1	0	0	1
	LT	0	1	1	0	0	0	0	1	1	1	1	0
	RT	0	0	1	0	0	0	0	0	0	0	1	0
3	TH	0	0	1	1	1	1	0	0	0	0	1	1
	LT	1	1	0	0	1	1	0	0	0	0	1	1
	RT	0	1	0	0	0	1	0	0	0	0	0	0
4	TH	0	1	1	0	0	1	1	1	1	0	0	0
	LT	0	1	1	1	1	0	0	1	1	0	0	0

Table 5: Summary of overall optimization results

		Number of variables			Number of	Computing		Reserved	Capacity
Intersection	Model	Binary	Integer	Continuous	Constraints	time (s)	μ	capacity	increase
1	Reference	92	0	86	898	2.48	1.3502	35.02%	-
	Proposed	336	144	86	2708	3.49	1.3656	36.56%	1.14%
2	Reference	104	0	106	1406	10.73	1.7983	79.83%	-
	Proposed	348	144	106	3112	9.61	1.9643	96.43%	9.23%
3	Reference	104	0	106	1406	7.22	1.7983	79.83%	-
	Proposed	360	144	106	3208	9.31	1.9643	96.43%	9.23%
4	Reference	116	0	126	2026	29.16	2.3129	131.29%	-
	Proposed	372	144	126	3612	16.63	2.6190	161.90%	13.23%

Table 6: Traffic performance measurement results

From arm	Lane	To arm (Assigned flow, veh/h) 1	2	3	4	Lane flow (veh/h)	Saturation flow (veh/h)	Capacity (veh/h)	Degree of saturation
Intersection 1 ($\mu = 1.3656$, cycle length = 90 s):									
	1			24	300	324	1633	471	0.6879
1	2			376		376	1900	548	0.6861
	3		200			200	1805	280	0.7143
	1	200			32	232	1649	329	0.7052
2	2				268	268	1900	380	0.7053
	3			200		200	1805	280	0.7143
	1		400			400	1615	1615	0.2477
3	2	200				200	1900	274	0.7299
	3				300	300	1805	441	0.6803
	1		32	200		232	1649	329	0.7052
4	2		268			268	1900	380	0.7053
	3	200				200	1805	280	0.7143
Intersection 2&3 ($\mu = 1.9643$, cycle length = 90 s):									
	1				300	300	1615	628	0.4777
1	2			204		204	1900	422	0.4834
	3		7	196		203	1897	421	0.4822
	4		193			193	1805	401	0.4813
	1	200				200	1615	771	0.2594
2	2				170	170	1900	358	0.4749
	3			38	130	168	1878	354	0.4746
	4			162		162	1805	340	0.4765
	1		400			400	1615	861	0.4646
3	2	172				172	1900	358	0.4804
	3	28			137	165	1820	343	0.4810
	4				163	163	1805	340	0.4794
	1			200		200	1615	1615	0.1238
4	2		170			170	1900	358	0.4749
	3	38	130			168	1878	354	0.4746
	4	162				162	1805	340	0.4765
Intersection 4 ($\mu = 2.6190$, cycle length = 90 s):									
	1				300	300	1615	1525	0.1967
	2			153		153	1900	422	0.3626
1	3			153		153	1900	422	0.3626
	4		55	95		150	1864	414	0.3623
	5		145			145	1805	401	0.3616
	1	200				200	1615	1309	0.1528
	2				128	128	1900	358	0.3575
2	3				128	128	1900	358	0.3575
	4			79	45	124	1838	347	0.3573

Continued on next page

Table 6 Continued: Traffic performance measurement results

From arm	Lane	To arm (Assigned flow, veh/h) 1	2	3	4	Lane flow (veh/h)	Saturation flow (veh/h)	Capacity (veh/h)	Degree of saturation
	5			121		121	1805	340	0.3559
	1		400			400	1615	1309	0.3056
	2	129				129	1900	358	0.3603
3	3	71			55	126	1857	350	0.3600
	4				122	122	1805	340	0.3588
	5				122	122	1805	340	0.3588
	1			200		200	1615	843	0.2372
	2		128			128	1900	358	0.3575
4	3		128			128	1900	358	0.3575
	4	79	45			124	1838	347	0.3573
	5	121				121	1805	340	0.3559